

Deposition of Silicon Nitride Thin Films by Hot-Wire CVD at 100°C and 250°C

P. Alpuim^{1*}, L.M. Gonçalves², E.S. Marins¹, T.M.R. Viseu³, S. Ferdov¹, J.E. Bourée⁴

¹Departamento de Física, Universidade do Minho, 4800-058 Guimarães, Portugal

²Departamento de Electrónica Industrial, Universidade do Minho, 4800-058 Guimarães, Portugal

³Departamento de Física, Universidade do Minho, 4710-057 Braga, Portugal

⁴Laboratoire de Physique des Interfaces et des Couches Minces, CNRS UMR 7647, Ecole Polytechnique, 91128 Palaiseau, France

Abstract

Silicon nitride thin films for use as passivation layers in solar cells and organic electronics or as gate dielectrics in thin-film transistors were deposited by the Hot-wire chemical vapor deposition technique at a high deposition rate (1-3 Å/s) and at low substrate temperature. Films were deposited using NH₃/SiH₄ flow rate ratios between 1 and 70 and substrate temperatures of 100°C and 250°C. For NH₃/SiH₄ ratios between 40 and 70, highly transparent ($T \sim 90\%$), dense films (2.56 - 2.74 g/cm³) with good dielectric properties and refractive index between 1.93 and 2.08 were deposited on glass substrates. Etch rates in BHF of 2.7 Å/s and <0.5 Å/s were obtained for films deposited at 100°C and 250°C, respectively. Films deposited at both substrate temperatures showed electrical conductivity $\sim 10^{-14} \Omega^{-1}\text{cm}^{-1}$ and breakdown fields $>10 \text{ MV cm}^{-1}$.

Keywords

Hot-wire CVD, silicon nitride, dielectric, low-temperature deposition, electronic transport

* Corresponding author.

1. Introduction

Silicon nitride is one of the most important dielectrics found in electronic technologies. It is used as state-of-the-art anti-reflection and surface passivation coating for crystalline silicon solar cells [1], as a passivation and mechanical protective layer in CMOS devices, as a mask for selective oxidation of silicon [2], and as a gate dielectric in amorphous silicon thin-film transistors. In recent years, it has become clear that the rapid advances achieved in the performance of entirely organic electronic devices were hampered by their instability under continued exposure to oxygen and moisture, even at extremely low concentrations [3]. Therefore, new stress-free, transparent and electrically insulating inorganic permeation barrier layers are requested in order to protect the devices and allow their market entrance. The maximum deposition temperature allowed for organic applications is below 150°C and often below 110°C. Silicon nitride barrier layers, if successfully deposited at such low temperatures, are good candidates to fulfill this task [4].

Typically, silicon nitride, SiN_x , has been deposited by radio-frequency plasma-enhanced chemical vapor deposition, rf-PECVD, at temperatures of ~400°C. We have studied deposition of SiN_x of electronic quality at 100°C by rf-PECVD, using silane and ammonia highly diluted in hydrogen (flow rate of hydrogen divided by total gas flow rate equal to 0.7) and a ratio of two between the flow rates of ammonia and silane [5].

Several groups have shown that the Hot-wire chemical vapor deposition technique, HWCVD, presented clear advantages over plasma-assisted deposition techniques for SiN_x deposition [6,7,8]. These advantages mainly result from the absence of ion bombardment during film growth, combined with a high efficiency for pyrocatalytic decomposition of the source gases, NH_3 and SiH_4 , on the filament surface. The rate of incorporation of nitrogen in the films depends

on the relative flow rates of NH_3 and SiH_4 (the dissociation probability of NH_3 on the heated filament is much less than that of SiH_4), and also on the working pressure in the chamber [8].

In this paper we show that dense, transparent SiN_x films with composition close to stoichiometry, with high electrical resistivity and breakdown field, are readily obtained by HWCVD at substrate temperatures of 250°C and 100°C , at a higher deposition rate than is achieved using the rf-PECVD technique, without the need for hydrogen dilution of the reactant gases.

2. Experimental

For HWCVD a single S-shaped tantalum filament ($d = 0.5$ mm, $l = 14$ cm) was heated up to 1750°C with a filament-to-substrate distance of 4.5 cm. The filament was first heated up to the working temperature, in a hydrogen atmosphere, and then the source gases, NH_3 and SiH_4 , were added while the hydrogen line was closed. Working gas pressure was 40 mTorr for all depositions. During the heating time, a shutter was moved to the closed position in order to protect the substrate from spurious species emitted from the filament. Two series of films were prepared on glass at $T_{\text{sub}} = 100^\circ\text{C}$ and 250°C , respectively. The substrate temperature was measured with a thermocouple embedded in the stainless steel substrate-holder, close to its surface. This means that, especially for the depositions made nominally at 100°C , the temperature of the film growing surface was certainly higher than the substrate-holder temperature due to heating from the hot filament and to H_2 formation from atomic hydrogen recombination at the film surface. Whenever the substrate temperature read at the Eurotherm display exceeded the nominal deposition temperature (110°C) by 10%, the deposition was stopped.

The ammonia-to-silane flow rate ratio, R , was varied between 1 and 70 in the first series, and between 40 and 70 in the second one. SiH_4 flow rate was 1 sccm for all depositions and NH_3 flow rate was varied to obtain the desired R -value. Optical transmittance of the films was measured with a UV-VIS-NIR spectrophotometer (Shimadzu UV 3100 PC) in order to determine their optical parameters. The value of the refractive index at 650 nm was used afterwards in the remaining part of the study. The etch rate was evaluated from the dependence of the thickness of the film (measured from transmittance spectra) on the immersion time in 10% buffered HF. Infrared spectra, which give information regarding the Si-H, N-H and Si-N bonds in the SiN_x films [9] were measured using the above-mentioned FT-IR spectrometer on samples deposited on double-polished $\langle 100 \rangle$ c-Si substrates. X-ray reflectometry (XRR) analyses were performed using a Bruker D8 Discover diffractometer operated in θ - θ geometry and equipped with a graded parabolic X-ray multilayer mirror. XRR intensities were recorded over 2θ angular range starting below the critical angle up to 2.5° with step size of 0.01° and using CuK_α radiation. The data from XRR were analyzed using the Leptos software package [10].

The thickness of the films was calculated from interference fringes of near-infrared optical transmission. Electrical measurements were made in a perpendicular geometry between evaporated Al contacts in a sandwich configuration. In order to make accurate electrical measurements, metal-insulator-metal, MIM, structures with contact areas $100 \times 100 \mu\text{m}^2$, $200 \times 200 \mu\text{m}^2$ and $400 \times 400 \mu\text{m}^2$ were fabricated using photolithography. The MIM structures are defined by the overlap of the Al contacts. Current-voltage curves were measured at different temperatures (between room temperature and 95°C) by applying a voltage between the top and the bottom contacts (at a rate of $\sim 1 \text{ V/s}$).

3. Results and discussion

Figure 1 shows the deposition rate, r_d , as a function of R for films deposited at 100°C and 250°C. Although the SiH_4 flow rate is constant for all depositions, r_d decreases as the NH_3 flow rate increases from 10 to 55 sccm and then stabilizes for $R > 70$. The trends in r_d versus R are similar for both temperatures with a lower r_d value for $T_{\text{sub}} = 100^\circ\text{C}$ compared to $T_{\text{sub}} = 250^\circ\text{C}$: for $R = 55$, $r_d = 1.0 \text{ \AA}/\text{s}$ for $T_{\text{sub}} = 100^\circ\text{C}$ and $1.3 \text{ \AA}/\text{s}$ for $T_{\text{sub}} = 250^\circ\text{C}$. This means that the limiting step in the growth mechanism at 100°C is the rate of incorporation of the precursors in the film.

Fig. 2 (left axis) shows the transmittance spectrum of sample SN308 (open circles) deposited at $T_{\text{sub}} = 100^\circ\text{C}$ and $R = 55$. This spectrum, when compared with that of the glass substrate (thin solid line), indicates that the film is highly transparent and that its band gap is higher than that of the glass. Thickness, and visible and near infrared optical parameters of the films were determined by fitting the measured transmittance spectra using the method described in reference [11]. The dispersion relation for the dielectric constant used in the parameterization from which the films' optical constants were obtained, is based on the classical Lorentz dielectric function $\tilde{\epsilon}(E)$:

$$\tilde{\epsilon}(E) = \epsilon_\infty + \frac{f E_0^2}{E_0^2 - E^2 + i\gamma_b E}$$

where ϵ_∞ is the high frequency dielectric constant, E_0 , γ_b and f are, respectively, the resonance energy frequency, the line-width and the strength of the Lorentzian oscillator, related to the bound electrons. From the fit of the transmittance data to the model, in the wavelength range 350-2000 nm, we obtained the thickness of 423 nm and the refractive index, n , shown in Fig. 2 (right axis). The value of n at 650 nm is 2.00, very close to the value 2.05 found in the literature for stoichiometric amorphous Si_3N_4 deposited at 450°C [2].

Fig. 3 shows the FT-IR spectra of the films deposited at 250°C in the *R*-series. It can be seen that, when *R* increases, so do the bands related to N–H vibrations (centered at ~1175 cm⁻¹ for the bending mode and at ~3330 cm⁻¹ for the stretching mode [9]), whereas the bands related to Si–H (2100-2200 cm⁻¹) decrease in size. Moreover, when *R* increases, the peak due to the Si–N stretching vibration, centered at ~830 cm⁻¹, shifts towards a higher wave number, signaling the strengthening of the Si-N bond. The structural feature that explains this shift is the increase in the number of N-H bonds and the decrease of Si-H bonds, when the films become more N-rich. Whenever one substitutes an H atom for a Si atom in the arrangement Si₂N-Si (giving SiHN-Si), the Si-N bond force constant increases due to the inductive effect that places more charge in between the two atoms. Conversely, whenever in the arrangement N₃Si-N one of the nitrogen atoms is replaced by H, the Si-N bond becomes weaker [12].

Fig. 4 shows the FT-IR peak position (left axis) of the Si-H stretching mode, as a function of *R*, for samples deposited at 100°C (open circles) and 250°C (solid squares). Fig.4 also shows the refractive index at 650 nm (right axis), as a function of *R*, for films deposited at 100°C (down triangles) and 250°C (up triangles). The position of the Si-H peak gives an indication of the N/Si atomic compositional ratio of the films [9] since it depends on the other bonds of the Si atom to which H is bonded to. According to reference [8], the shift of the Si-H peak position is proportional to the N/Si ratio in the layers up to 2200 cm⁻¹ obtained for N/Si = 1.2. For N/Si > 1.2 this relation is no longer valid. If one combines this information with the value of *n* close to 2.05 exhibited by the films deposited at *R* = 40 and 55, one concludes that their composition should be close to stoichiometry.

XRR was performed on thin films (*d*~50 nm) deposited at 100°C and 250°C using *R* = 55, to measure very accurately their thickness (*d* = 47.3 and 49.8 nm, respectively) and check the

deposition rates, and on thicker films ($d > 200$ nm) in order to measure their density and roughness. From the fitting to the data [13], one obtains a density of 2.56 and 2.74 g/cm³ for the films deposited at $T_{\text{sub}} = 100^\circ\text{C}$ and 250°C , respectively. For both films, the roughness is equal (1.6 nm), within experimental error. The etch rate in BHF for these films (see Table I) was 2.7 Å/s and < 0.5 Å/s, respectively, which are the smaller etch rate values found at each temperature. Fig. 5 shows that the films obtained at $R = 55$ and $T_{\text{sub}} = 100^\circ\text{C}$ or 250°C have the lowest electrical conductivity as a function of R , respectively $\sigma = 6.7 \times 10^{-14} \Omega^{-1} \text{cm}^{-1}$ and $\sigma = 1.2 \times 10^{-14} \Omega^{-1} \text{cm}^{-1}$. These values are in the typical range of device quality SiN_x deposited at high substrate temperature. It is interesting to point out that at $T_{\text{sub}} = 100^\circ\text{C}$ it was not possible to obtain films with correct stoichiometry ($\text{N/Si} = 1.33$) using rf-PECVD (see ref. [5]), since the films were either Si-rich or N-rich. On the other hand, the dielectric breakdown field of such films was ~ 10 MVcm⁻¹. In the present work, electric fields nominally (voltage divided by film thickness) of 20 MVcm⁻¹ were not enough to disrupt the films deposited using $R = 55$ and 70. In films deposited by rf-PECVD at 100°C , at a given value of the electric field, the I versus V behavior became super-linear, following a power law regime. The conductivity was thermally activated for N-rich films and independent of temperature, for Si-rich films.

In films deposited at 100°C or 250°C using HWCVD, none of this complex behavior can be observed (see inset in Fig.5), and the conductivity is constant for electric fields in the range from -20 MV.cm⁻¹ to $+20$ MV.cm⁻¹. This behavior also rules out, in the range of temperature and E-field studied, conduction mechanisms controlled by space-charge limited currents, such as Poole-Frenkel, a strongly temperature dependent mechanism, which are associated with a large density of electron trapping states in the dielectric.

4. Conclusions

Device quality silicon nitride films have been deposited at $T_{\text{sub}} = 100^\circ\text{C}$ and 250°C from silane and ammonia gaseous mixtures by the HWCVD technique at a higher growth rate than comparable films deposited by rf-PECVD. For NH_3/SiH_4 ratios between 40 and 70, highly transparent ($T \sim 90\%$), dense films with good dielectric properties and refractive index between 1.93 and 2.08 were obtained. For $\text{NH}_3/\text{SiH}_4 = 55$, densities of 2.56 and 2.74 g/cm^3 were obtained for the films deposited at $T_{\text{sub}} = 100^\circ\text{C}$ and 250°C , as well as an electrical conductivity of $\sim 10^{-14} \Omega^{-1}\text{cm}^{-1}$ and a breakdown field $>10 \text{ MV}\cdot\text{cm}^{-1}$. Etch rates in BHF of 2.7 $\text{\AA}/\text{s}$ and $<0.5 \text{ \AA}/\text{s}$ were measured for films deposited at 100°C and 250°C , respectively. Electrical conduction is ohmic in a wide range of temperatures (20°C to 95°C) and electric fields (up to $20 \text{ MV}\cdot\text{cm}^{-1}$).

Acknowledgements

This work was partly supported by the CNRS/ Fundação para a Ciência e Tecnologia (FCT) program under contract no. 20798. One of the authors (E. Marins) acknowledges FCT for a research grant under project PTDC-CTM-66558-2006.

References

- [1] B. Hoex, A.J.M. van Erven, R. C. M. Bosch, W.T.M. Stals, M. D. Bijker, P.J. van den Oever, W.M.M. Kessels, M.C.M. van de Sanden, Prog. Photovolt: Res. Appl. 13 (2005) 705.
- [2] H.C. Cheng, in: C.Y. Chang and S.M. Sze (Eds.), ULSI Technology, Chapter 5, McGraw-Hill International Editions, Singapore, 1996, p.205.
- [3] H. Chatham, Surf. Coat. Technol. 78 (1996) 1.
- [4] J. Ubrig, PhD Thesis, Ecole Polytechnique (2007) <http://de.scientificcommons.org/28161998>
- [5] P. Alpuim, P. Ferreira, V. Chu, J.P. Conde, J. Non-Cryst. Solids, 299-302 (2002) 434.
- [6] H. Matsumura, J. Appl. Phys. 66 (1989) 3612.
- [7] A. H. Mahan, Thin Solid Films, 501 (2006) 3.
- [8] V. Verlaan, Z.S. Houweling, C.H.M. van der Werf, I.G. Romijn, A.W. Weeber, H.D. Goldbach, R.E.I. Schropp, Thin Solid Films, 516 (2008) 533.
- [9] E. Bustarret, M. Bensouda, M.C. Habrard, J.C. Bruyère, S. Poulin, S.C. Gujrathi. Phys. Rev. B 38 (1988) 8171.
- [10] LEPTOS version 4.03, available from Bruker-AXS, Karlsruhe, Germany.
- [11] D.A. Minkov, J. Phys. D: Appl. Phys. 22 (1989) 199.
- [12] R.C. Budhani, S. Prakash, H.J. Doerr, R.F. Bunshah, J. Vac. Sci. Technol. A5 (1987) 1644.
- [13] M. Wormington, "A Novel Method for Automated Fitting of X-ray Scattering Data", presented at the 48th Annual X-ray Conference, Denver, August 1999.

List of tables and figures

Table I. Properties of selected SiN_x samples deposited by HWCVD at $T_{\text{sub}}=100^{\circ}\text{C}$ and 250°C .

Fig. 1. Deposition rate, r_d , as a function of the flow rate ratio of NH₃ to SiH₄, R , for substrate temperatures of 100°C and 250°C . (The lines are guides to the eye.)

Fig. 2. Left axis: measured (open circles) and simulated (red line) transmittance spectra of sample SN308, deposited at $T_{\text{sub}}=100^{\circ}\text{C}$ and $R=55$. The spectrum of the glass substrate (thin solid line) is also shown for comparison. Right axis: refractive index (blue line) deduced from the transmittance data in the wavelength range 300-2000 nm.

Fig. 3. Fourier-transform infrared transmission spectra of the films in the R -series (R is NH₃/SiH₄ flow rate ratio) deposited at 250°C . The small numbers placed next to each spectrum indicate the corresponding value of R .

Fig. 4. The Si-H stretching mode peak position (left axis), as a function of the flow rate ratio NH₃/SiH₄ of process gases, R . Refractive index at 650 nm is plotted as a function of R (right axis).

Fig. 5. Room-temperature electrical conductivity of the SiN_x films deposited at $T_{\text{sub}}=100^{\circ}\text{C}$ (squares) and 250°C (triangles) as a function of R . Insert shows series of I - V curves measured at temperatures between 25°C and 95°C on sample deposited at $T_{\text{sub}}= 100^{\circ}\text{C}$ and $R=55$.

Table I

Sample	T_{sub} (°C)	R	d (nm)	r_d (Å/s)	Si-H peak position (cm^{-1})	n ($\lambda = 650 \text{ nm}$)	Etch rate in BHF (Å/s)	σ ($\Omega^{-1} \text{ cm}^{-1}$)
SN240	250	1	150	5.00	2072			
SN239	250	10	200	2.60	2122			1.0×10^{-9}
SN238	250	20	135	2.25	2151			2.2×10^{-11}
SN244	250	40	321	1.78	2198	2.08	<0.5	
SN243	250	55	235	1.30	2213			1.2×10^{-14}
SN242	250	70	220	1.22	2222	1.93		2.2×10^{-12}
SN720	100	20	250	1.69*	2160	2.06		
SN247	100	40	330	1.38	2198	2.07	<5.0	4.0×10^{-13}
SN308	100	55	423	1.00	2200	2.00	2.7	6.7×10^{-14}
SN309	100	70	577	1.00	2211	1.94	3.5	1.0×10^{-12}

* filament-to-substrate distance = 7 cm

Figure 1

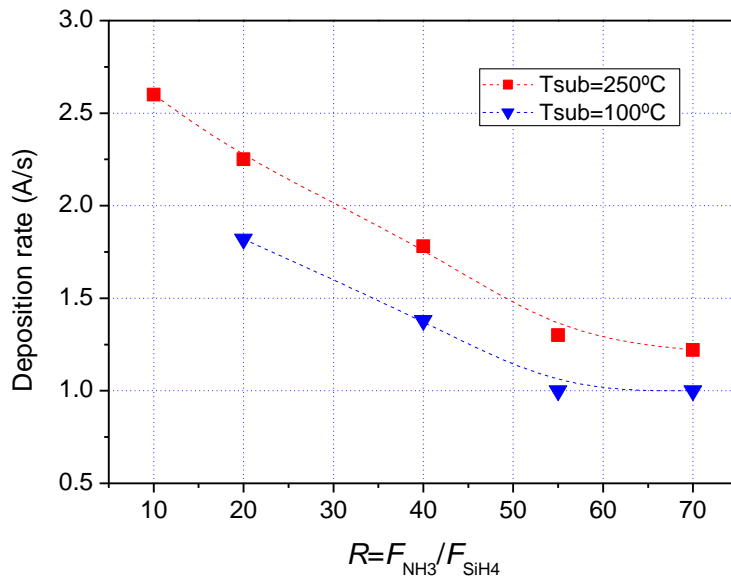


Figure 2

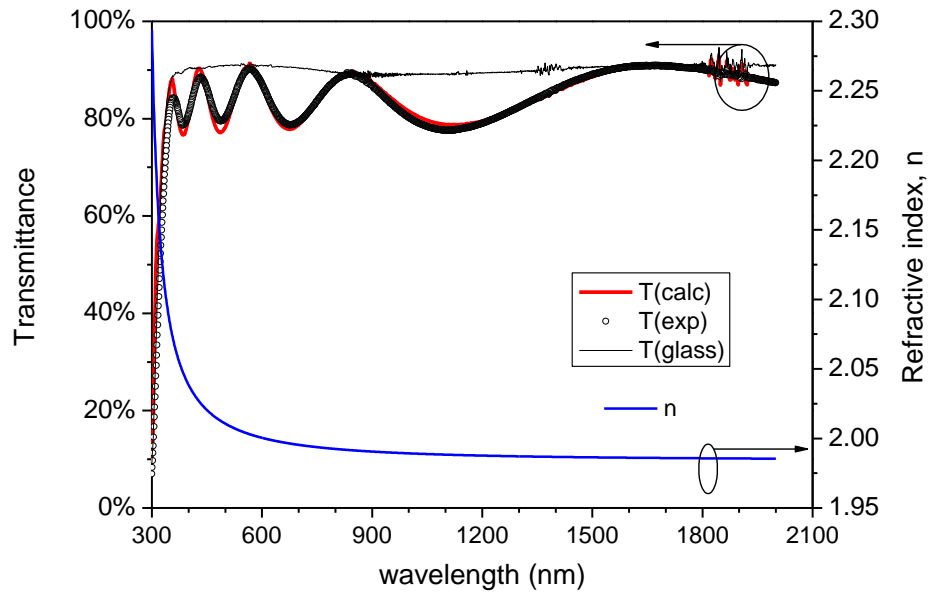


Figure 3

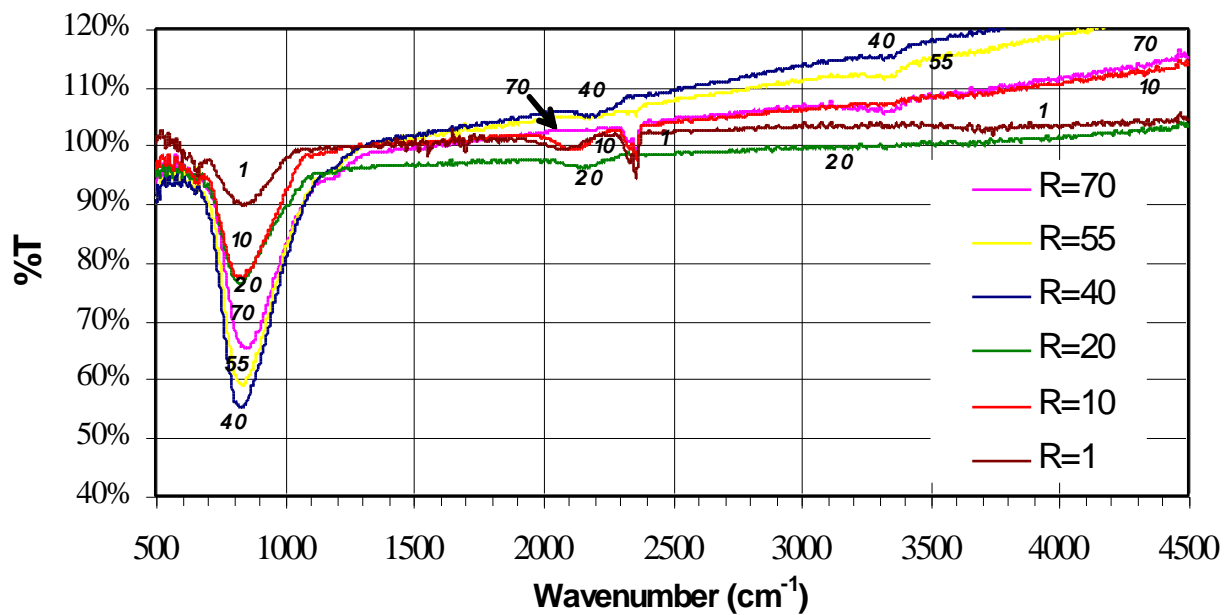


Figure 4

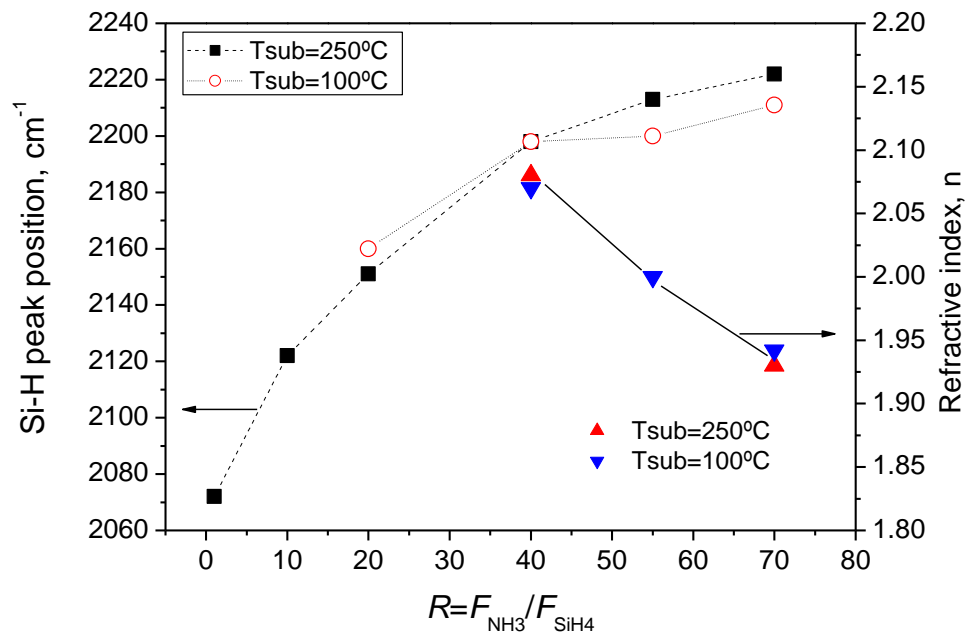


Figure 5

